

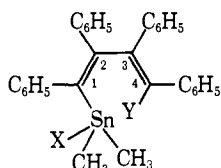
## A Study of the Rotational Process in Sterically Hindered Dienes

F. P. Boer, G. A. Doorakian, H. H. Freedman, and S. V. McKinley

*Contribution from The Dow Chemical Company, Eastern Research Laboratory, Wayland, Massachusetts 01778. Received June 25, 1969*

**Abstract:** The temperature-dependent nmr spectra of the diastereotopic methyl protons of (4-halo-1,2,3,4-tetraphenyl-1,3-butadienyl)dimethyltin halides (I–III) and (4-halo-1,2,3,4-tetraphenyl-1,3-butadienyl)dimethylphenyltins (V–VII) have been studied to determine activation energies for interchange between enantiomeric conformations of these dissymmetric skewed dienes. These studies afford the first opportunity to measure directly rotational barriers in 1,3-dienes. Enhanced rates of methyl exchange in I–III in the presence of electron-donating solvents have been shown to arise by an independent mechanism believed to involve inversion of configuration at tin. The structure of (4-bromo-1,2,3,4-tetraphenyl-*cis,cis*-1,3-butadienyl)dimethyltin bromide (II) has been determined by a single-crystal X-ray diffraction study. This compound crystallizes in space group P2<sub>1</sub>/c,  $a = 14.805$ ,  $b = 18.619$ ,  $c = 13.589$  Å,  $\beta = 131.20^\circ$ , and  $Z = 4$ . The structure was refined by full-matrix least squares to a reliability index  $R_1 = 0.107$  for 1609 reflections above background. This diene is found to be skewed  $68.1^\circ$  from the planar *s-cis* geometry. The molecular geometry also provides novel structural evidence for an intramolecular Sn–Br interaction (3.774 Å), where the bromine bonded to the carbon 4 of the diene acts as an electron donor to pentacoordinate tin.

Our interest in the ground-state conformational properties of the tin-substituted tetraphenyl dienes, I–IV, was prompted by the observation<sup>1,2</sup> that all but one of these compounds exhibited a temperature (and/or solvent) dependent nmr spectrum as revealed by the reversible coalescence of magnetically nonequivalent methyl substituents on tin. In a preliminary



- I, X = Cl; Y = Cl  
 II, X = Br; Y = Br  
 III, X = I; Y = I  
 IV, X = I; Y = H  
 V, X = C<sub>6</sub>H<sub>5</sub>; Y = Cl  
 VI, X = C<sub>6</sub>H<sub>5</sub>; Y = Br  
 VII, X = C<sub>6</sub>H<sub>5</sub>; Y = I

communication<sup>2</sup> we proposed that a rotational barrier was responsible for this behavior and that this barrier was a direct result of hindered rotation in a skewed diene stabilized by an internal tin–halogen interaction. Additional rate and solvent data on I–IV, as well as similar studies on three new dienes (V–VII), have enabled us to elaborate on the source and energetics of the barriers and to distinguish clearly between two independent processes for methyl exchanges.

Our studies of the kinetics of methyl interchange afford the first opportunity to measure directly the rotational barrier about the central bond of a 1,3-diene. Concurrently, information has also been obtained on factors affecting the inversion of configuration at tetrahedral tin.

## Nmr Exchange Measurements

The proton magnetic resonance spectra of seven tetraphenylbutadienyltin compounds (I–VII) have been

- (1) H. H. Freedman, *J. Org. Chem.*, **27**, 2298 (1962).  
 (2) F. P. Boer, J. J. Flynn, H. H. Freedman, S. V. McKinley, and V. R. Sandel, *J. Amer. Chem. Soc.*, **89**, 5068 (1967).

examined in carbon tetrachloride solution. Two equal intensity methyl resonances were observed at room temperature for all compounds except IV, where Y = H. The coalescence of the two signals to a single peak upon heating indicates rapid exchange of the methyl environments. Rates of exchange over a range of temperatures were measured by matching experimental spectra with computer-generated curves calculated<sup>3</sup> according to the equations of Kubo<sup>4</sup> and Sack.<sup>5</sup> Figure 1 shows sample comparison spectra for V; exchange rates determined as a function of temperature for I–III, V, and VI are plotted in Figure 2. Activation energies and their standard deviations were obtained by a least-squares fit to these data; their values, along with coalescence temperatures  $T_c$  and chemical shift separations  $|\nu_A - \nu_B|$ , are given in Table I. Free energies, enthalpies, and entropies of activation were derived in the usual manner from the Eyring equation.

Separate methyl signals could not be resolved for IV even at  $-80^\circ$ . This result is believed to be consistent with a substantially lower activation barrier than observed in the other compounds of the series, although a considerably reduced value of  $|\nu_A - \nu_B|$  could also account for this observation.

## Conformation of the Diene

The molecular structure of II has been determined by single-crystal X-ray diffraction methods. The molecular geometry is shown in Figures 3 and 4, and selected bond distance and bond angle data are given in Tables II and III. The severe skew of the diene from a planar conformation is probably best seen in the three-dimensional drawing,<sup>6</sup> Figure 4, which views the molecule down the C(2)–C(3) diene single bond. The degree of skew can be measured by the angle between the planes of the two ethylenic moieties, as defined by a least-squares fit<sup>7</sup> to the two doubly bonded carbons and the

(3) We thank George Whitesides for the use of his computer program, EXCHLO, which solves the basic eq 24 described in H. O. House, R. A. Latham, and G. M. Whitesides, *J. Org. Chem.*, **32**, 2495 (1967).

(4) R. Kubo, *Nuovo Cimento, Suppl.*, **6**, 1063 (1957).

(5) R. A. Sack, *Mol. Phys.*, **1**, 163 (1958).

(6) ORTEP is a FORTRAN thermal ellipsoid plot program by C. K. Johnson, Oak Ridge National Laboratory, Oak Ridge, Tenn.

**Table I.** Activation Parameters, Coalescence Temperatures, and Chemical Shifts for Substituted Tetraphenylbutadienylytins in  $\text{CCl}_4$  Solution<sup>a</sup>

Compound	X	Y	$E_a$	$\Delta F \ddagger_{25^\circ}$	$\Delta H \ddagger_{25^\circ}$	$\Delta S \ddagger_{25^\circ}$ , eu	$T_c^\circ$ , C	$ \nu_A - \nu_B $
I	Cl	Cl	$17.0 \pm 0.3$	16.8	$16.4 \pm 0.3$	$-1.4 \pm 1.0$	60	20.8
II	Br	Br	$18.3 \pm 0.2$	18.0	$17.7 \pm 0.2$	$-1.0 \pm 0.7$	87	30.0
III	I	I	$22.6 \pm 1.1$	19.7	$22.1 \pm 1.1$	$7.9 \pm 3$	(106) <sup>b</sup>	36.8
V	$\text{C}_6\text{H}_5$	Cl	$17.6 \pm 0.2$	17.8	$17.0 \pm 0.2$	$-2.6 \pm 0.7$	66	12.0
VI	$\text{C}_6\text{H}_5$	Br	$19.0 \pm 0.7$	18.6	$18.4 \pm 0.7$	$-0.9 \pm 2$	85	14.2
VII	$\text{C}_6\text{H}_5$	I					96	16.2

<sup>a</sup> Energy units are in kilocalories per mole, chemical shifts are in hertz at 60 MHz. <sup>b</sup>  $T_c$  was estimated from extrapolation of Arrhenius plot to  $k$  ( $\text{sec}^{-1}$ ) at coalescence where  $k_c \approx \pi(\nu_A - \nu_B)/\sqrt{2}$ .

four atoms directly attached (see Table IV, planes E and F). The dihedral angle thus defined is  $68.1^\circ$  from the planar *s-cis* conformation. The phenyl groups are all twisted well out of coplanarity with the double bonds: phenyl rings A and B form dihedral angles  $69.4$  and  $59.2^\circ$  with plane E and rings C and D form angles of  $52.4$  and  $49.1^\circ$  with plane F (see again Table IV). Thus, conjugation effects between the  $\pi$  systems of this molecule appear to be minimal.

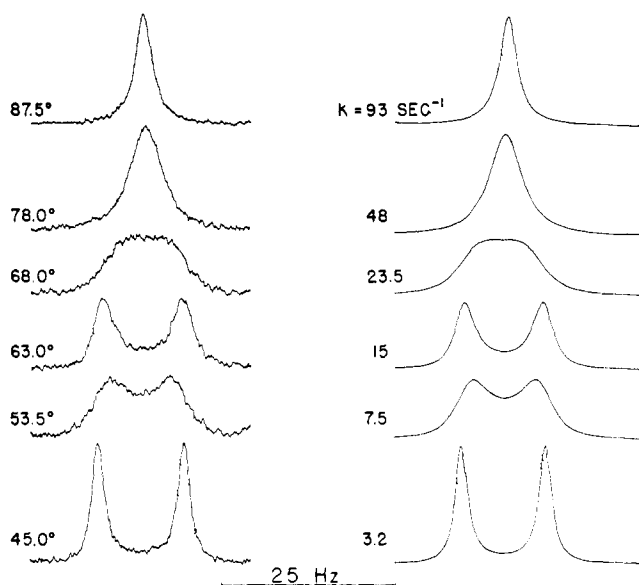


**Figure 1.** Observed and calculated nmr spectra of methyl protons of (4-chloro-1,2,3,4-tetraphenyl-*cis,cis*-1,3-butadienyl)dimethylphenyltin(V) in carbon tetrachloride.

Such a highly skewed structure is not surprising in view of the steric restrictions imposed on this hindered 1,3-diene. Models for the planar *s-cis* and *s-trans* conformations (Figure 5) drawn by computer from standard bond distance and angle data<sup>8</sup> indicate that both these geometries are precluded by severe steric repulsions. The  $68.1^\circ$  skew angle found in our X-ray study must be near the lower limit for this system, since the distances between substituents on carbons 1 and 4 are already inside the van der Waals limits; *vide infra*.

(7) J. Gvildys, "Least-Squares Plane and Line Fitter," ANL Program Library B-125; see V. Schomaker, J. Waser, R. E. Marsh, and G. Bergman, *Acta Crystallogr.*, **12**, 600 (1959).

(8) L. E. Sutton, "Tables of Interatomic Distances and Configuration in Molecules and Ions," Special Publication No. 11, The Chemical Society, London, 1958.

**Table II.** Bond Distances ( $\text{\AA}$ )<sup>a</sup>

Sn-Br(1)	2.504 (5)	C(13)-C(14)	1.436 (30)
Sn-Br(2)	3.774 (5)	C(14)-C(15)	1.370 (31)
Sn-C(1)	2.206 (21)	C(15)-C(16)	1.356 (32)
Sn-C(5)	2.150 (22)	C(16)-C(17)	1.381 (33)
Sn-C(6)	2.195 (24)	C(17)-C(18)	1.468 (31)
		C(18)-C(13)	1.398 (30)
C(4)-Br(2)	1.952 (22)	C(19)-C(20)	1.437 (32)
C(1)-C(2)	1.377 (26)	C(20)-C(21)	1.378 (31)
C(2)-C(3)	1.460 (27)	C(21)-C(22)	1.461 (32)
C(3)-C(4)	1.449 (28)	C(22)-C(23)	1.372 (32)
		C(23)-C(24)	1.496 (30)
C(1)-C(7)	1.394 (24)	C(24)-C(19)	1.379 (30)
C(2)-C(13)	1.447 (29)		
C(3)-C(19)	1.458 (27)	C(25)-C(26)	1.409 (28)
C(4)-C(25)	1.489 (26)	C(26)-C(27)	1.438 (31)
		C(27)-C(28)	1.409 (34)
C(7)-C(8)	1.357 (27)	C(28)-C(29)	1.409 (34)
C(8)-C(9)	1.494 (31)	C(29)-C(30)	1.596 (36)
C(9)-C(10)	1.450 (32)	C(30)-C(25)	1.323 (32)
C(10)-C(11)	1.296 (30)		
C(11)-C(12)	1.525 (28)		
C(12)-C(7)	1.374 (38)		

<sup>a</sup> Standard deviations calculated from the variance-covariance matrix obtained in the final least-squares cycle are given in parentheses.

**Table III.** Selected Bond Angles<sup>a,b</sup>

C(1)-Sn-Br(1)	100.7 (0.5)	C(1)-C(2)-C(3)	125.7 (2.2)
C(5)-Sn-Br(1)	100.0 (0.7)	C(1)-C(2)-C(13)	121.0 (2.1)
C(6)-Sn-Br(1)	105.1 (0.7)	C(3)-C(2)-C(13)	113.2 (2.0)
C(1)-Sn-C(5)	129.0 (0.8)		
C(1)-Sn-C(6)	105.9 (0.8)	C(2)-C(3)-C(4)	125.5 (2.1)
C(5)-Sn-C(6)	112.7 (0.9)	C(2)-C(3)-C(19)	117.2 (2.0)
		C(4)-C(3)-C(19)	116.6 (2.0)
Br(2)-Sn-Br(1)	149.5 (0.1)		
Br(2)-Sn-C(1)	66.2 (0.5)	C(3)-C(4)-Br(2)	116.7 (1.6)
Br(2)-Sn-C(5)	72.4 (0.7)	C(3)-C(4)-C(25)	128.8 (2.1)
Br(2)-Sn-C(6)	105.1 (0.7)	Br(2)-C(4)-C(25)	114.4 (1.6)
Sn-C(1)-C(2)	122.7 (1.6)		
Sn-C(1)-C(7)	115.0 (1.4)		
C(2)-C(1)-C(7)	121.9 (2.1)		

<sup>a</sup> Central atom is vertex. <sup>b</sup> Standard errors calculated from the variance-covariance matrix are given in parentheses.

Though the most stable conformation of the molecule in solution may not be exactly that found in the solid state, a high degree of dissymmetry must exist for any conformation with reasonable intramolecular contacts.

The methyl groups, as located in the X-ray study, have distinctly different chemical environments; one is near phenyl A, the other is in contact with Br(2). As seen in Figure 6, both enantiomeric conformations of II exist in the crystal, related by the inversion centers and glide planes of the space group.

Table IV

	A. Least-Squares Planes <sup>a</sup>					
	Plane A	Plane B	Plane C	Plane D	Plane E	Plane F
Atom 1	C(1)	C(2)	C(3)	C(4)	Sn	Br(2)
Atom 2	C(7)	C(13)	C(19)	C(25)	C(1)	C(2)
Atom 3	C(8)	C(14)	C(20)	C(26)	C(2)	C(3)
Atom 4	C(9)	C(15)	C(21)	C(27)	C(3)	C(4)
Atom 5	C(10)	C(16)	C(22)	C(28)	C(7)	C(19)
Atom 6	C(11)	C(17)	C(23)	C(29)	C(13)	C(25)
Atom 7	C(12)	C(18)	C(24)	C(30)		
$m_1$	8.597	2.410	4.708	7.099	-7.856	13.954
$m_2$	12.892	-0.948	15.801	13.911	10.433	6.019
$m_3$	-0.820	8.617	-7.168	0.414	11.251	-9.298
$d$	0.835	0.448	1.219	1.248	3.600	-2.743
$\Delta d$ (atom 1)	0.006	-0.008	-0.050	-0.075	-0.028	-0.037
$\Delta d$ (atom 2)	-0.001	0.022	0.062	0.012	-0.041	0.014
$\Delta d$ (atom 3)	-0.008	-0.024	0.017	0.033	0.005	0.056
$\Delta d$ (atom 4)	-0.004	0.000	-0.025	0.035	0.053	0.001
$\Delta d$ (atom 5)	0.018	0.032	0.003	-0.073	0.063	-0.058
$\Delta d$ (atom 6)	-0.013	-0.046	-0.024	-0.023	-0.052	0.024
$\Delta d$ (atom 7)	0.001	0.023	0.016	0.092		

B. Dihedral Angles between Least-Squares Planes			
Plane 1	Plane 2	Angle, deg	
A	E	69.4	
B	E	59.2	
C	F	52.4	
D	F	49.1	
E	F	68.1	

<sup>a</sup> These planes are defined by the equation  $m_1x + m_2y + m_3z = d$ . The distances  $\Delta d$  of the atoms from this plane are in Å.

Except for concurrent work on 1-halo and 1,4-dihalo-substituted tetraphenylbutadienes,<sup>9</sup> relatively few structures of hindered 1,3-dienes have been established directly. One of the few published examples describes

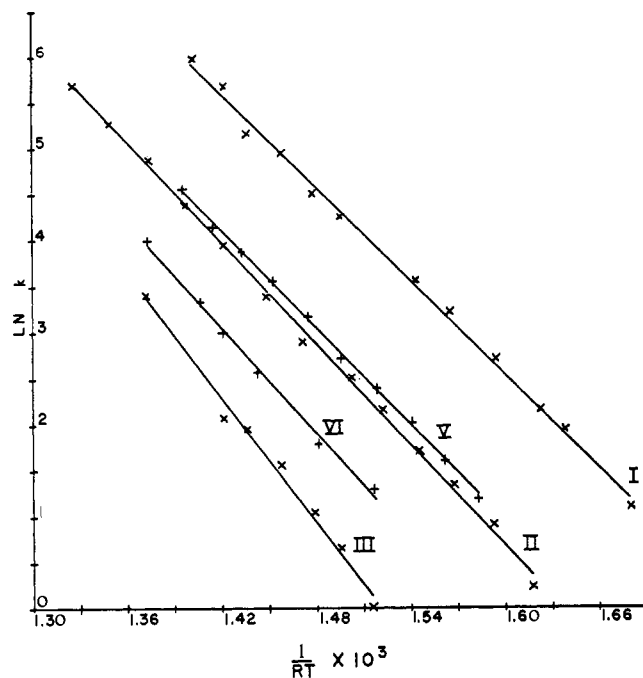


Figure 2. Arrhenius plots of  $\ln k$  ( $\text{sec}^{-1}$ ) as a function of  $1/T$  for I, II, III, V, and VI.

a calciferol derivative where a  $54^\circ$  dihedral angle from planar *s-cis* was found.<sup>10</sup> The importance of 1,3-

(9) G. A. Doorakian, H. H. Freedman, R. F. Bryan, and H. P. Weber, *J. Amer. Chem. Soc.*, **92**, 399 (1970).

diene conformation in influencing the rate of Diels-Alder additions has been well established<sup>11</sup> and recent results on the rates of electrocyclic ring closure of hindered dienes to cyclobutenes suggest that ground-state conformational preference is a critical factor here as well.<sup>9</sup>

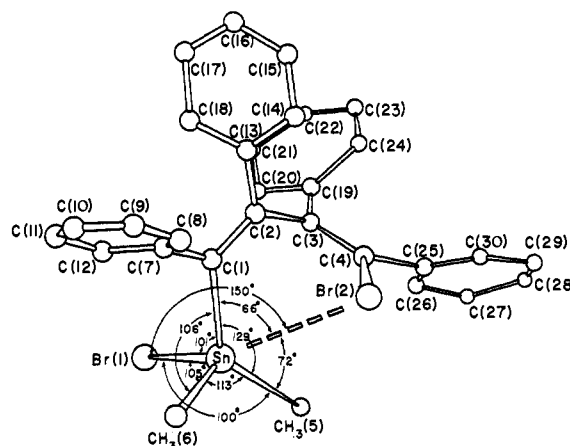


Figure 3. View of a (4-bromo-1,2,3,4-tetraphenyl-*cis,cis*-1,3-butadienyl)dimethyltin bromide molecule indicating the numbering system and showing bond angles at tin.

### Origin of the Methyl Nonequivalence

In a formal sense at least, coalescence of nonequivalent methyl resonances in I-III and V-VII may arise from several possible types of conformational changes, which may be divided broadly into two groups. In group A, both methyl groups of a given conformation are diastereomeric with respect to their environments

(10) D. C. Hodgkin, B. M. Rimmer, J. D. Dunitz, and K. N. Trueblood, *J. Chem. Soc.*, 4945 (1963).

(11) J. G. Martin and R. K. Hill, *Chem. Rev.*, **61**, 537 (1961).

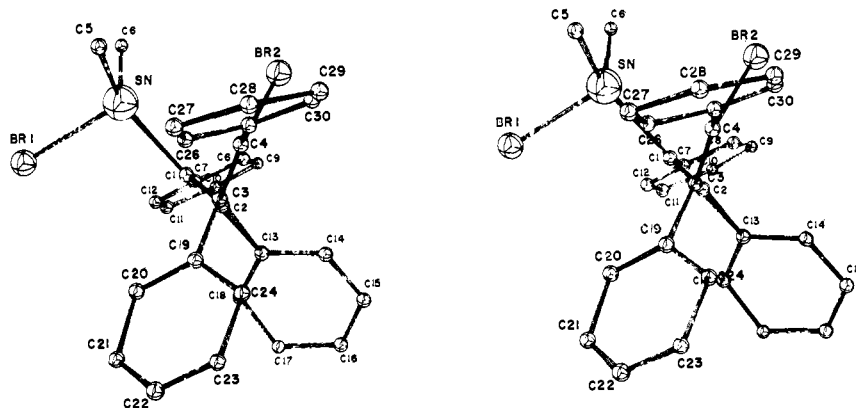


Figure 4. Three-dimensional drawing of (4-bromo-1,2,3,4-tetraphenyl-*cis,cis*-1,3-butadienyl)dimethyltin bromide (II) as viewed in a direction approximately along the diene single bond, C(2)–C(3). The diene skew angle and the intramolecular Sn···Br interaction are readily seen in this view.

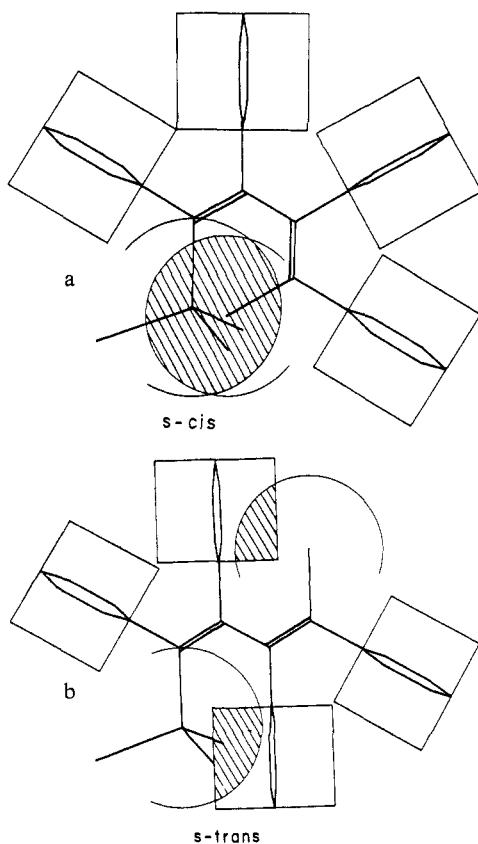


Figure 5. Computer generated drawings of planar transition states for (4-bromo-1,2,3,4-tetraphenyl-*cis,cis*-1,3-butadienyl)dimethyltin bromide (II). The molecular coordinates were generated assuming  $120^\circ$  bond angles at carbon,  $109.5^\circ$  angles at tin, and bond lengths C–C, 1.466; C=C, 1.335; C–C (phenyl), 1.396; Sn–C, 2.163; Sn–Br, 2.510; and Br–C, 1.875 Å. The circles represent van der Waals radii of 2.2 Å at tin and 1.95 Å at bromine, and the boxes represent the 3.4 Å thickness of an aryl ring. No attempt was made to represent the 2.0 Å van der Waals radii of the methyl groups. Areas where these regions overlap are shaded.

in their alternative conformation(s). Under these conditions the rotamers are unrelated by any symmetry elements and must in principle have different energies. Group B defines interchange of diastereotopic<sup>12</sup> methyls

(12) K. Mislow and M. Raban, "Stereoisomeric Relationships of Groups in Molecules" in "Topics in Stereochemistry," Vol. 1, N. L. Allinger and E. L. Eliel, Ed., Interscience Publishers, New York, N. Y., 1967.

between conformers that are either enantiomeric or identical. The only mechanism that will be shown to be consistent with the data presented above, *i.e.*, hindered rotation about the diene single bond, belongs to this second group, but we consider it worthwhile to examine all of the possibilities in turn. Processes involving interchange of chemically distinct conformations (group A) may be further subdivided into types, according to whether the distinct rotamers are defined with respect to the C(2)–C(3) bond ( $A_1$ ) or the Sn–C(1) bond ( $A_2$ ).

Process  $A_1$ , the simpler example of the first type, involves planar *s-cis* and *s-trans* diene conformations where each methyl singlet represents both methyls of a particular rotamer. However, the experimentally observed peaks are of equal intensity, and this implies nearly equal populations of the two rotamers in all compounds over a wide temperature range, a situation which we regard as highly unlikely. These planar diene conformations are also obviously prohibited on steric grounds (Figure 5). The more complex case of exchange between nonplanar (dissymmetric) rotamers implies the existence of at least four separate methyl resonances arising from diastereotopic groups existing within individual diastereomers.<sup>12</sup> This interpretation, particularly if extended to all compounds of the series, requires an unreasonable amount of coincidence of chemical shifts and/or populations to account for the observed data.

Mechanism  $A_2$  considers hindered rotation about the Sn–C(1) bond while assuming the butadiene chain to be locked in a dissymmetric conformation. These conditions maintain *intrinsic dissymmetry*, which is analogous to intrinsic asymmetry as described for ethane-type molecules.<sup>13</sup> Even if the methyl groups reside equally in each of several possible rotational conformations, the average environments can never be exactly identical, and the chemical shifts of the inherently diastereotopic methyls will never be averaged. The fact that the chemical shift differences for I–III and V–VII range from 12 to 36 Hz and exhibit minor temperature dependence below coalescence suggests that a measurable change in rotamer populations probably does not occur. Thus, mechanism  $A_2$  is supposititious and need not be considered further.

(13) M. van Gorkom and G. E. Hall, *Quart. Rev.*, **32**, 19 (1968).

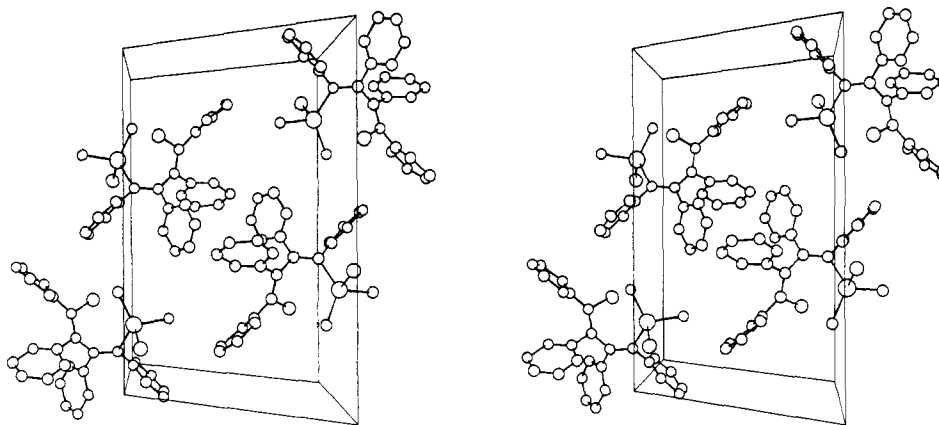
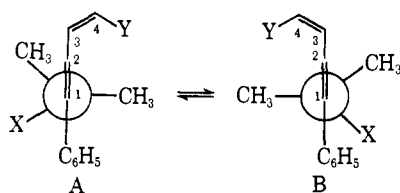


Figure 6. Stereo-pair drawing of molecular packing in (4-bromo-1,2,3,4-tetraphenyl-*cis,cis*-1,3-butadienyl)dimethyltin bromide (II). The *y* axis is vertical, and we are viewing approximately down *z*. Among the shorter intermolecular contact are Br(1)···Br(2), 3.977; Br(1)···C(18), 3.832; and Br(2)···CH<sub>3</sub>(5), 3.956 Å. The shortest intermolecular C···C contact is 3.44 Å.

Two types of interchange of diastereotopic methyls between identical or enantiomeric conformations (group B) may be considered. Inversion of configuration at tin, while the butadienyl ligand retains its chirality (mechanism B<sub>1</sub>), leads to an optically identical conformation in which the methyls have been exchanged. Such inversion could result, for example, by ionization of halide leading to a trigonal-planar transition state geometry at tin. The absence of a significant effect on rates of thermal equilibration noted<sup>2</sup> when studies were carried out in a strongly ionizing medium, thionyl chloride, militated against this interpretation. In any case, the new data for the tetraorganotin series V–VII (where ionization is not feasible and the barriers are nearly identical with their analogs I–III) rules out an ionization mechanism.

Finally, mechanism B<sub>2</sub> pertains to interconversion of enantiomers, which in general requires concomitant rotation about the Sn–C(1) and C(2)–C(3) bonds, as illustrated in projection view of A ⇌ B



Presuming that these processes require significantly different activation energies, we can assume that the barrier to one of these rotations is being measured, while the other, at least in relative terms, is facile. Our experimental data allow us to identify which of these barriers is rate determining. Under the assumption of facile C(2)–C(3) rotation, the effect of the Y substituent on a rate-determining Sn–C(1) rotation barrier should be negligible. On the contrary, the observed barriers increase in the known order of steric size, H << Cl < Br < I, as Y is varied. Similarly, changing the size of the X substituent at tin should be reflected in the Sn–C(1) rotational barrier but the data in Table I do not support this assertion. We therefore conclude that this experiment measures barriers to rotation about the diene single bond, and that barriers to rotational isomerization at tin are not relevant.

### Source of the Barrier

The presence of restricted rotation about the diene single bond has led us to consider two alternate sources for the observed barrier arising, respectively, from repulsive and attractive interactions. Steric repulsions in the *s-cis* and *s-trans* transition state of II are portrayed in Figures 5a and b. The degree to which normal van der Waals distances must be penetrated to achieve these transition states obviously requires the expenditure of considerable energy. On the basis of these computer-drawn models, the *s-trans* form is expected to be the favored transition state. The relative inaccessibility of the more sterically hindered *s-cis* transition state may be reflected in the pyrolysis reactions of dienes I–III: the formation of cyclobutadiene from II by the thermal extrusion of (CH<sub>3</sub>)<sub>2</sub>SnBr<sub>2</sub> has been postulated to occur *via* a *cisoid* transition state and requires an *E*<sup>‡</sup> of 24 kcal/mol,<sup>14</sup> in contrast to the 18.4-kcal barrier observed here.

The observed reduction of the barrier as the steric size of Y is reduced is clearly consistent with the steric interactions in the favored transition state (Figure 5b). Moreover, we would expect X substituents to have negligible effect on the barrier since X can be rotated out of the crowded region. The fact that the barriers (Table I) are virtually unchanged when phenyl is substituted for halogen at X, for a given Y substituent, supports this reasoning.

Our previous speculation<sup>2</sup> that the barrier might be influenced by a weak attractive Sn–Y interaction has now been shown to be invalid. This hypothesis was originally suggested by the X-ray structure of II, which provided structural evidence for a weak Sn–Br bond, and appeared to be consistent with the effects of Lewis bases (*vide infra*). Compounds V–VII were designed specifically to clarify this point, since tin compounds of the type SnR<sub>3</sub>X (X = halogen) are known to form coordination complexes with electron donors, whereas no such complexes are known for SnR<sub>4</sub>.<sup>15</sup> On this basis the substantial decrease in the Sn–Y interaction would be expected to be paralleled by a concomitant decrease in the rotational barrier; in fact the barriers

(14) V. R. Sandel and H. H. Freedman, *J. Amer. Chem. Soc.*, **90**, 2059 (1968).

(15) I. R. Beattie, *Quart. Rev.*, **17**, 382 (1963).

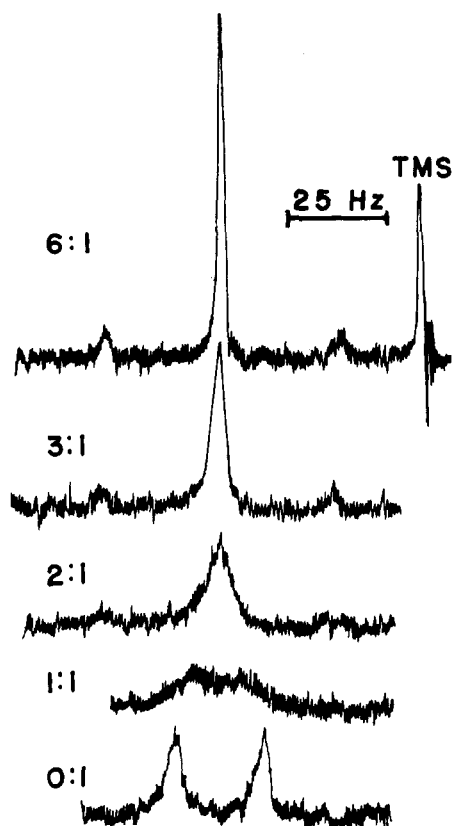


Figure 7. Nmr spectra of the methyl protons of (4-bromo-1,2,3,4-tetraphenyl-*cis,cis*-1,3-butadienyl)dimethyltin bromide (II) in  $\text{CDCl}_3$  at  $36^\circ$  in which the molar ratio of pyridine to II is varied as indicated. Tin-methyl couplings are distinguishable in the upper spectra as small satellites flanking the main band.

are completely insensitive to substitution of phenyl for halogen at X. Furthermore, preliminary X-ray diffraction data<sup>16</sup> on VI show no unusual Sn-Br interactions of the type found in II. We conclude that Sn-Y interactions which may be present in I-III are insufficiently energetic to account for the observed thermal barriers. The geometry of these molecules requires that these weak Sn-Y bonds be broken well before the diene has rotated to the maximum energy *s-trans* configuration.

#### Coordination Effects at Tin

If internal tin-halogen bonding is irrelevant to the thermal barriers, alternate mechanisms for the effect<sup>2</sup> of Lewis bases on the methyl exchange must be considered. The observation that addition of Lewis bases to solutions of II was effective in restoring methyl equivalence, even at  $36^\circ$ , was noted previously.<sup>2</sup> Methyl exchange as a function of molar proportion of Lewis base is seen in Figure 7 for II in  $\text{CDCl}_3$ , where the concentration of pyridine is varied and the temperature is constant. Additional studies on compounds I-III indicate that the order of effectiveness of bases in restoring methyl equivalence qualitatively parallels the known order of nitrogen base strength, aliphatic amine > aniline  $\approx$  pyridine, as well as the order found for coordinate bond strength, dimethylformamide > pyridine, in studies<sup>17</sup> of trimethyltin chloride complexes.

(16) F. P. Boer and F. P. van Remoortere, unpublished results.

(17) T. F. Bolles and R. S. Drago, *J. Amer. Chem. Soc.*, **88**, 5730 (1966).

Our present studies also suggest that aliphatic alcohols are surprisingly effective in this respect.

In contrast to these results, the methyl resonances of the tetraorganotin compounds V-VII are completely unaffected by the presence of Lewis bases and remain unchanged even in neat pyridine.

The intermolecular coordination effects observed above have their intramolecular counterpart, as determined by the X-ray diffraction data on II and VI. The molecular structure of II gives an intramolecular Sn-Br(2) distance of  $3.774 \pm 0.005 \text{ \AA}$  (Table II), an amount approximately  $0.4 \text{ \AA}$  less than the sum of tin and bromine van der Waals radii.<sup>18</sup> Although the van der Waals concept should be applied with caution to intramolecular distances, there is some additional evidence that the Sn-Br interaction in II is at least weakly bonding. As discussed above, Lewis bases are known to bond to triorganotin halides<sup>19</sup> but not to tetraorganotin and a Sn-Br bond would therefore not be expected to form in VI, where X =  $\text{C}_6\text{H}_5$  instead of X = Br. In fact the Sn-Br distance in VI is more than  $4.3 \text{ \AA}$ , well above the van der Waals limit.<sup>16</sup> Because II and VI should have essentially the same steric requirements, there is little to recommend any argument that the short Sn-Br interaction in II results from steric compression in other parts of the molecule. Weak Sn-Br forces probably stabilize the *cisoid* skew structure found for II, and somewhat different, but undoubtedly non-planar, conformations may exist in the absence of this interaction.

Additional evidence for an attractive interaction in II is the dramatic opening of the C(1)-Sn-CH<sub>3</sub>(5) angle to  $129.0 \pm 0.8^\circ$ , approximately  $20^\circ$  more than the normal tetrahedral angle. Other angles in the system (Figure 3 and Table III) have correspondingly narrowed to make room for the Sn-Br contact. We note parenthetically that to describe the structure in terms of either of the common geometries for pentacoordinate species,<sup>20</sup> *i.e.*, a trigonal bipyramid<sup>19</sup> or a tetragonal pyramid, would be inaccurate. The Br(1)-Sn-Br(2) angle deviates from the linearity expected of a trigonal bipyramid by a full  $30^\circ$  and the space for the extra interaction is provided essentially by widening of the C(1)-CH<sub>3</sub>(5) edge of the coordination tetrahedron. Direct evidence for intramolecular tin-halogen coordination, a relatively novel phenomenon, has also been presented<sup>21</sup> recently for  $\text{bipy}(\text{OC})_3\text{ClMoSnCH}_3\text{Cl}_2$ .

The previously noted identity of the barriers in I-III with V-VII and the absence of base effects on the methyl exchange of V-VII rule out the possibility that diene single-bond rotation is involved in the base-catalyzed exchange processes in I-III. Instead, we believe these latter processes to occur *via* an entirely different mechanism, in which inversion at tin, rather than loss of diene chirality, gives rise to an exchange of methyl groups that is rapid on the nmr time scale. Although relatively little information is available on the

(18) The radius for Br is taken as  $1.95 \text{ \AA}$  (L. Pauling, "The Nature of the Chemical Bond," 3rd ed, Cornell University Press, Ithaca, N. Y., 1960, p 263). The radius for Sn,  $2.2 \text{ \AA}$ , is estimated by extrapolating the values of neighboring elements (Sb, Te, I) on the periodic chart (see p 260), or alternatively by using the heuristic rule (p 263):  $r(\text{van der Waals}) = 0.8 + r(\text{single bond})$ .

(19) R. Hulme, *J. Chem. Soc.*, 1524 (1963).

(20) M. Gielen and N. Sprecher, *Organometal. Chem. Rev.*, **1**, 455 (1966); review of pentacoordination in group IV compounds.

(21) M. Elder, W. A. G. Graham, D. Hall, and R. Kummer, *J. Amer. Chem. Soc.*, **90**, 2189 (1968).

configurational stability of tin, a mechanism formally similar to  $B_1$  above appears reasonable in the presence of coordinating base. In fact, such a mechanism has been proposed for the group IV element silicon by Sommer and coworkers,<sup>22</sup> in which base-catalyzed racemization of optically resolved  $R_3SiF$  is believed to proceed through a tetragonal-pyramidal transition state. An analogous square-pyramidal transition state, with Lewis base at the apex, could occur in I-III. In general any transition state where the four ligands ( $R_3$  and halogen) become instantaneously coplanar can invert the tin configuration and exchange methyls. This study is one of the few examples where a diastereotopic probe can be applied to quantitative measurements of configurational stability at tin in the presence of various coordinating ligands. In a related study, Peddle and Redl<sup>23</sup> have demonstrated that the addition of small amounts of the coordinating bases, acetone or DMSO, coalesces the diastereotopic methyls in an  $R_3SnX$  compound,  $\beta,\beta$ -dimethylphenethylmethylphenyltin chloride,<sup>23a</sup> but does not affect the  $R_4Sn$  compound  $\beta$ -methyl- $\beta$ -phenethylmethylphenyltin.<sup>23b</sup>

Finally, the  $^{117,119}Sn-CH_3$  coupling constants provide support for the presence of base coordination in the series I-III and its absence in V-VII (see Table V).  $J$  values<sup>24</sup> for the two methyl signals of V-VII in  $CCl_4$  fall between 52.4 and 54.0 Hz.  $J$  values for I-III in  $CCl_4$  are slightly higher, 53.2-58.7 Hz. A similar difference occurs (Table V) when the simpler tetraor-

are found in V and VI, consistent with our previous conclusion that bases coordinate readily with the former but not the latter compounds.

## Experimental Section

**I. Syntheses.** (4-Chloro-1,2,3,4-tetraphenyl-*cis,cis*-1,3-butadienyl)dimethyltin chloride (I), (4-bromo-1,2,3,4-tetraphenyl-*cis,cis*-1,3-butadienyl)dimethyltin bromide (II), and (4-iodo-1,2,3,4-tetraphenyl-*cis,cis*-1,3-butadienyl)dimethyltin iodide (III) were prepared as described in ref 1.

**(4-Halo-1,2,3,4-tetraphenyl-*cis,cis*-1,3-butadienyl)dimethylphenyltin Compounds.** These were all prepared by reaction of the corresponding (4-halo-1,2,3,4-tetraphenyl-*cis,cis*-1,3-butadienyl)dimethyltin halide with approximately 2 equiv of phenylmagnesium bromide (Arapahoe Chemicals) at 0°. The solvent used for the preparation of the chloro and bromo derivatives was tetrahydrofuran (dried over  $CaH_2$ ) and for the iodo derivative, diethyl ether (dried over  $CaH_2$ ). The crude solids were recrystallized from methylene chloride-ethanol mixture and gave products in approximately 85% yield. The chloro derivative (V) was a white solid with mp 149-150°. (*Anal.* Calcd for  $C_{36}H_{31}ClSn$ : C, 69.99; H, 5.06; Cl, 5.74; Sn, 19.21. Found: C, 69.75; H, 5.14; Cl, 5.84; Sn, 19.27 by difference.) The bromo derivative (VI) was a white solid with mp 159-161°. (*Anal.* Calcd for  $C_{36}H_{31}BrSn$ : Br, 12.07; Sn, 17.92. Found: Br, 12.30; Sn, 17.95.) The iodo derivative (VII) was a pale yellow solid with mp 146.5-148°. (*Anal.* Calcd for  $C_{36}H_{31}ISn$ : C, 60.96; H, 4.41; I, 17.89; Sn, 16.74. Found: C, 60.78; H, 4.42; I, 17.89; Sn, 16.91 by difference.)

**(1,2,3,4-Tetraphenyl-*cis,cis*-1,3-butadienyl)dimethyltin Iodide (IV).** The corresponding chloride was refluxed 72 hr in acetone in the presence of excess NaI. Extraction from the acetone residue into methylene chloride and recrystallization from ethanol gave light yellow rectangular prisms of mp 158-160°. (*Anal.* Calcd for  $C_{30}H_{27}ISn$ : I, 20.04; Sn, 18.75. Found: I, 20.15; Sn, 18.53.) The physical properties of the starting chloride, obtained as a reaction by-product, were reported in ref 1; however an alternate synthesis by addition of 1 equiv of dry HCl in  $CH_2Cl_2$  to dimethylstannole<sup>1</sup> gave this chloride in 80% yield.

**II. Nmr Measurements. a. Kinetic Studies.** The kinetic parameters reported in Table I were all obtained on ~2 to 10% (by weight) solutions of the butadienyltin compounds in  $CCl_4$ . The nmr measurements were obtained at 60 MHz on a Varian A56/60 spectrometer equipped with variable-temperature probe and temperature controller. Typically, spectra were recorded in duplicate at a sweep width of 2 Hz/cm and the amplitude of the radiofrequency field was kept below the level where saturation effects could be observed. Theoretically calculated line shapes were found to accurately reproduce the observed spectra, and rates of methyl exchange between magnetically nonequivalent sites were obtained from a comparison of experimental spectra to computed spectra. The calculations were performed using either EXCH10<sup>3</sup> on an IBM 7094 computer or a modified version of this program on an IBM 1130 and plotted using a Calcomp plotter. Values for  $T_2$ , the relaxation times of the protons in the absence of exchange, were obtained from the slow exchange limit spectra. Care was taken over the entire temperature range to assure constant optimum homogeneity by use of internal TMS. Temperature was measured using standard ethylene glycol or methanol samples. The temperature range covered for rate measurements for all compounds was approximately 40-70° except in the case of III in which only the range of exchange broadening below coalescence was accessible in  $CCl_4$  solvent. In this case fewer spectra were recorded over a shorter temperature range and this is reflected in larger least-squares errors in the activation parameters. The approximate coalescence temperature was obtained by extrapolation to the temperature at which  $k = \pi\delta\nu/\sqrt{2}$  where  $\delta\nu$  equals the separation in hertz between the peaks.

**b. Coupling Constants.** The coupling constants,  $J^{119}Sn-CH_3$  and  $J^{117}Sn-CH_3$ , were obtained by the usual side-band calibration technique using a Hewlett Packard audiooscillator and frequency counter. In most cases the  $^{117}Sn-CH_3$  and  $^{119}Sn-CH_3$  couplings were clearly resolvable. However, for convenience the reported  $J$  is the average of the  $^{117}Sn-CH_3$  and  $^{119}Sn-CH_3$  coupling, and in comparison to literature values the average  $J$  is also used.

**c. Chemical Shifts.** Chemical shifts from TMS of the two methyl resonances for  $CCl_4$  solutions of I-III and V-VII are as follows: I ( $\delta = 0.78, 0.43$ ), II ( $\delta = 0.98, 0.48$ ), III ( $\delta = 1.26, 0.65$ ), V ( $\delta = 0.43, 0.20$ ), VI ( $\delta = 0.47, 0.23$ ), and VII ( $\delta = 0.53, 0.26$ ). The single methyl resonance of IV appears at  $\delta = 0.85$ .

Table V. Tin-Methyl Couplings (Hz) in  $CCl_4$  and Pyridine<sup>a</sup>

Compound	X		$CCl_4$		Pyridine	
	X	Y	$CH_3^b$	$CH_3^c$	$CH_3^b$	$CH_3^c$
I	Cl	Cl	55.8	53.2	64.6	
II	Br	Br	58.7	54.6	63.0	
III	I	I	58.3	54.4		
V	$C_6H_5$	Cl	53.9	53.3	53.9	53.2
VI	$C_6H_5$	Br	53.0	52.4	54.8	53.2
VII	$C_6H_5$	I	54.0	53.5		
$(CH_3)_3SnCl$				57.3 <sup>d</sup>		66.2
$(CH_3)_4Sn$				52.6 <sup>d</sup>		53.2

<sup>a</sup> See ref 24. Solutions were ~2-10% by weight. Measurements were made at probe temperature (~36°) except for I and V in  $CCl_4$  (~10°). Estimated error is  $\pm 0.7$  Hz. <sup>b</sup> Coupling associated with lower field methyl resonance. <sup>c</sup> Coupling associated with higher field methyl resonance. <sup>d</sup> J. R. Holmes and H. D. Kaesz, *J. Amer. Chem. Soc.*, **83**, 3903 (1961).

ganotin compound  $Sn(CH_3)_3$ ,  $J = 52.6$  Hz, is compared to the triorganotin halide,  $Sn(CH_3)_3Cl$ ,  $J = 57.3$  Hz. This effect has been ascribed to redistribution of s character in the bonds as a result of the introduction of the more electronegative ligand.<sup>17, 25</sup> When  $Sn(CH_3)_3Cl$  is dissolved in pyridine, the  $J$  value increases markedly to 66.2 Hz, an effect attributed<sup>17</sup> to the formation of an adduct with a nearly trigonal-bipyramidal structure. A similar increase to 63-64.6 Hz is observed for  $J$ (pyridine) in I and II, but no changes in  $J$  values

(22) L. H. Sommer and P. G. Rodewald, *J. Amer. Chem. Soc.*, **85**, 3898 (1963).

(23) (a) G. J. D. Peddle and G. Redl, *Chem. Commun.*, 626 (1968); (b) G. Redl and G. J. D. Peddle, Abstracts, Fourth International Conference on Organometallic Chemistry, Bristol, England, 1969, B9. We are grateful to a referee for pointing out this very recent reference.

(24) The  $^{117}Sn-CH_3$  and  $^{119}Sn-CH_3$  coupling constants were clearly resolved in all cases except one but for conciseness we report the average of the two, here denoted simply as  $J$ .

(25) P. B. Simons and W. A. G. Graham, *J. Organometal. Chem.*, **8**, 479 (1967).

d. Lewis Base Effects. Survey experiments designed to determine qualitatively the order of effectiveness of Lewis bases in restoring methyl equivalence were performed by titrating aliquots of base into solutions of known concentrations of II in  $\text{CCl}_4$  and recording the methyl peaks at a constant temperature. The approximate quantities of base required to produce comparable exchange-broadened spectra were as follows: benzylamine ( $\ll 1$  equiv), triethylamine ( $\ll 1$  equiv), dimethylformamide ( $< 1$  equiv), pyridine (2 equiv in  $\text{CDCl}_3$ ), aniline (5 equiv), and methanol (5 equiv).

III. X-Ray Data Collection. Single crystals of I can be grown from *t*-butyl alcohol as needles with hexagonal cross sections. For the diffraction study we chose crystals with approximate radii of 0.03 mm and with cross sections tending as closely as possible to regular hexagons. Unfortunately, the crystals deteriorated gradually in the X-ray beam, with noticeable yellowing and loss of diffracted intensity.

Photographs taken on a Weissenberg goniometer, with the long *c* axis of the crystal aligned parallel to the spindle, showed a reciprocal lattice symmetry  $\text{C}_{2h}$  and the systematic absence of  $0k0$  reflections for *k* odd and  $h0l$  for *l* odd, thus establishing space group  $\text{P2}_1/\text{c}$ . The crystal was then transferred to a Picker automatic diffractometer, carefully centered, and aligned with the real *c* axis parallel to  $\phi$ . Lattice constants were calculated by least-squares refinement of the setting angles of ten reflections using  $\text{Cu K}\alpha$  radiation ( $\lambda$  1.5418 Å). The unit cell dimensions  $a = 14.805 \pm 0.012$ ,  $b = 18.619 \pm 0.028$ ,  $c = 13.589 \pm 0.006$  Å, and  $\beta = 131.20 \pm 0.08^\circ$ , give a density  $\rho = 1.567$  g  $\text{cm}^{-3}$  for  $\text{C}_{30}\text{H}_{26}\text{SnBr}_2$ , and  $Z = 4$ .

The intensity data were collected using the  $2\theta$  scan mode of the diffractometer with Ni-filtered  $\text{Cu K}\alpha$  radiation. The X-ray tube was set at a  $3^\circ$  take-off angle, and a detector aperture 4.0-mm square was placed 30 cm from the crystal. Scan angles from 1.9 to  $2.6^\circ$  were employed over the range (0–106°) of  $2\theta$  examined. The scan speed was  $1^\circ/\text{min}$ . Background counts of 15 sec were taken at each end of the scan by the stationary-crystal-stationary-counter technique. The net intensity  $I = N_0 - kN_b$  of each reflection was assigned an initial error  $\sigma(I) = [(0.05I)^2 + N_0 + k^2N_b]^{1/2}$  where  $N_0$  was the gross count,  $N_b$  the background count, and  $k$  the ratio of scan time to background time. Reflections for which  $\sigma(I)/I > 0.25$ , or for which the net count was negative, were regarded as absent and omitted from the refinement. These constituted about half the total number of reflections measured. A rough correction for the decomposition of the crystals in the X-ray beam was made by continuously rescaling the data to previous test reflections; whenever the test reflections had diminished in intensity by 20% this effect was judged too serious for further correction and the crystals were discarded.

Absorption corrections were applied to the data assuming that the crystals were ideal cylinders aligned parallel to the  $\phi$  axis of the diffractometer. Under this assumption, the crystal axis forms an angle  $\psi$  with both the direct and diffracted beams, where  $\psi = \sin^{-1}(1/t)$ ,  $t$  is defined as  $(1 - \sin^2 \chi \sin^2 \theta)^{-1/2}$ , and  $\chi$  and  $\theta$  are the conventional diffractometer angles. Then the corrected intensities are given by

$$I^{\text{corr}} = \frac{I}{t \sum \Delta s e^{-\mu R g}}$$

where  $R$  is the cylinder radius and  $\mu$  is the linear absorption coefficient of the crystal at the wavelength used (in this case  $\mu = 112.7$   $\text{cm}^{-1}$ ). The quantity  $g$  is the reduced path length associated with a fraction of the cylinder cross section  $\Delta s$ ; tables of  $g$  and  $\Delta s$  have been calculated by Bond<sup>26</sup> as a function of  $\theta'$ , where  $2\theta'$  is the angle formed by the projections of the direct and diffracted beams on a plane perpendicular to the cylinder axis, i.e.,  $\theta' = \frac{1}{2}[\cos^{-1} \{t^2(1 - 2 \sin^2 \theta + \sin^2 \chi \sin^2 \theta)\}]$ . In the present study absorption factors varied by 10%.

Because of the deterioration problem, the intensity data were collected from four different crystals. The four data sets were correlated and merged using the program DIFCOR.<sup>27</sup> Of the total of 3179 independent reflections measured 1570 were discarded as absent. Of the remaining 1609 observed reflections, there were 1100 overlaps between the four data sets. The disagreement factor between the data sets was 11%, with a noticeable tendency toward poorer agreement among the low intensity reflections.

(26) W. L. Bond, *Acta Crystallogr.*, **12**, 375 (1959).

(27) J. Hartsuck, Harvard University.

Table VI. Atomic Parameters<sup>a</sup>

Atom	<i>x/a</i>	<i>y/b</i>	<i>z/c</i>	<i>B</i>
Sn	0.04363 (16)	0.19444 (9)	0.16759 (17)	
Br(1)	0.08035 (40)	0.13442 (22)	0.03185 (42)	
Br(2)	-0.17349 (27)	0.25856 (16)	0.20597 (27)	
C(1)	-0.0443 (18)	0.1067 (11)	0.1864 (19)	4.64 (50)
C(2)	-0.1670 (20)	0.1022 (12)	0.1090 (20)	5.38 (54)
C(3)	-0.2546 (19)	0.1524 (12)	0.0056 (21)	5.90 (58)
C(4)	-0.2764 (20)	0.2246 (13)	0.0255 (21)	6.13 (60)
C(5)	-0.0307 (20)	0.2946 (12)	0.0646 (22)	6.26 (59)
C(6)	0.2222 (22)	0.2069 (13)	0.3619 (23)	7.81 (72)
C(7)	0.0335 (18)	0.0610 (11)	0.2925 (20)	4.77 (51)
C(8)	0.0428 (19)	0.0610 (12)	0.3987 (22)	5.86 (57)
C(9)	0.1248 (23)	0.0141 (15)	0.5161 (26)	8.52 (74)
C(10)	0.1922 (21)	-0.0303 (13)	0.4964 (24)	7.05 (67)
C(11)	0.1881 (20)	-0.0363 (12)	0.3985 (23)	6.19 (60)
C(12)	0.1018 (21)	0.0151 (14)	0.2854 (23)	7.20 (66)
C(13)	-0.2216 (22)	0.0424 (13)	0.1213 (22)	6.53 (63)
C(14)	-0.3053 (23)	0.0523 (13)	0.1404 (22)	6.79 (64)
C(15)	-0.3549 (22)	-0.0061 (15)	0.1506 (24)	7.27 (65)
C(16)	-0.3269 (24)	-0.0731 (16)	0.1391 (25)	7.92 (69)
C(17)	-0.2564 (25)	-0.0880 (14)	0.1086 (25)	7.94 (70)
C(18)	-0.1953 (21)	-0.0268 (14)	0.1064 (22)	7.06 (66)
C(19)	-0.3393 (22)	0.1244 (12)	-0.1274 (22)	6.21 (60)
C(20)	-0.2907 (24)	0.0855 (16)	-0.1748 (27)	8.65 (79)
C(21)	-0.3671 (25)	0.0514 (15)	-0.2943 (27)	8.80 (76)
C(22)	-0.4959 (23)	0.0578 (14)	-0.3688 (23)	7.30 (69)
C(23)	-0.5520 (25)	0.0900 (14)	-0.3308 (27)	8.59 (77)
C(24)	-0.4617 (22)	0.1250 (12)	-0.2001 (22)	6.59 (62)
C(25)	-0.3643 (20)	0.2787 (11)	-0.0740 (22)	5.44 (56)
C(26)	-0.3699 (22)	0.2862 (13)	-0.1811 (24)	6.88 (66)
C(27)	-0.4604 (25)	0.3355 (15)	-0.2797 (25)	7.82 (69)
C(28)	-0.5390 (26)	0.3674 (15)	-0.2676 (28)	9.09 (80)
C(29)	-0.5267 (27)	0.3615 (17)	-0.1560 (30)	10.08 (90)
C(30)	-0.4199 (25)	0.3118 (16)	-0.0408 (26)	8.60 (76)

Anisotropic Thermal Parameters ( $\times 10^4$ )<sup>b</sup>

	Sn	Br(1)	Br(2)
$\beta_{11}$	128 (2)	322 (7)	177 (4)
$\beta_{22}$	37 (1)	76 (2)	49 (1)
$\beta_{33}$	182 (3)	408 (9)	172 (4)
$\beta_{12}$	0 (1)	-7 (3)	11 (2)
$\beta_{13}$	91 (2)	292 (7)	110 (3)
$\beta_{23}$	4 (1)	-20 (3)	-7 (2)

<sup>a</sup> Standard errors are given in parentheses. <sup>b</sup> The anisotropic thermal parameters are defined by  $T = \exp[-(\beta_{11}h^2 + \beta_{22}k^2 + \beta_{33}l^2 + 2\beta_{12}hk + 2\beta_{13}hl + 2\beta_{23}kl)]$ .

IV. Solution and Refinement of the Crystal Structure. The solution of the crystal structure was straightforward. The tin and bromine atoms were located in a normal-sharpened three-dimensional Patterson function calculated<sup>26</sup> from a preliminary data set of 1137 independent reflections. Two cycles of least-squares refinement<sup>28</sup> of the positions and isotropic temperature of these three atoms reduced  $R_1 = \sum |F_o| - |F_c| / \sum |F_o|$  from 0.40 to 0.33. The thirty carbon atoms were then located in an electron density map<sup>29</sup> from which the Sn and Br atoms had been subtracted. Four cycles of isotropic refinement of all 33 atoms reduced  $R_1$  to 0.147. Some of the structural parameters at this stage of the refinement have been reported in a preliminary communication.<sup>2</sup> An additional intensity data set was collected subsequently, and then merged and correlated with the previous data. Also, eight low-order high-intensity reflections (100, 110, 011, 111, 012, 112, 202, and 302) that were suspected of extinction were dropped from the data set, resulting in a final set of 1601 reflections. A correction for anomalous scattering<sup>30</sup> from the tin and bromine atoms was introduced, and refinement was continued assuming anisotropic

(28) (a) Least-squares and structure factor calculations were performed using ANAL-FLS-14E, J. Gvildy's version of Busing, Martin and Levy's OR-FLS. (b) Atomic scattering factors were taken from "International Tables for X-Ray Crystallography," Vol. III, The Kynoch Press, Birmingham, England, 1962, p 201.

(29) Fourier calculations were performed using program B-149 (Argonne National Laboratory), a version of Shoemaker, Sly, and Van der Hende's ERFR-2 by J. Gvildy.

(30) "International Tables for X-Ray Crystallography," Vol. III, The Kynoch Press, Birmingham, England, pp 214-215.



**Table VII.** Root-Mean-Square Displacements Along the Principal Axes of the Thermal Ellipsoids and Direction Cosines of the Principal Axes Referred to  $a$ ,  $b$ , and  $c^*$

Atom	Axis	Displacement <sup>a</sup>	Direction Cosines		
Sn	1	0.255 (3)	0.104	0.991	-0.085
	2	0.284 (3)	-0.732	0.018	-0.681
	3	0.333 (3)	-0.673	0.133	0.728
Br(1)	1	0.331 (5)	0.756	-0.553	0.348
	2	0.373 (5)	-0.575	-0.816	0.049
	3	0.481 (5)	0.312	-0.164	0.936
Br(2)	1	0.271 (4)	-0.408	0.825	0.391
	2	0.307 (3)	-0.146	0.363	-0.920
	3	0.360 (5)	0.901	0.432	0.027

<sup>a</sup> Standard errors are given in parentheses.

thermal parameters for Sn and Br and isotropic for C. Four cycles of full-matrix least squares reduced  $R_1$  to 0.107 and  $R_2 = (\sum w(|F_o| - |F_c|)^2 / \sum w F_o^2)^{1/2}$  to 0.131. The mean parameter shift in the final cycle was 0.009  $\sigma$  with a maximum shift of 0.05  $\sigma$ . A final electron-density difference map revealed no peaks greater than 1.4 e/Å<sup>3</sup> (and no peaks larger than 0.8 e/Å<sup>3</sup> apart from the regions occupied by the heavy atoms). In our judgment the structure was insufficiently overdetermined to justify further refinement with anisotropic thermal parameters for carbon.

The observed and calculated structure factors have been deposited<sup>31</sup> with the ASIS National Auxiliary Publication Service, New York, N. Y., as Document No. NAPS-00809. Table VI lists the final atomic parameters and their standard deviations. The root-mean-square displacements along the principal axes of the thermal ellipsoids, and the direction cosines of these axes, were computed from the anisotropic thermal parameters of the tin and bromine atoms; these are compiled in Table VII. Bond distances, with standard errors calculated<sup>32</sup> from the variance-covariance matrix obtained in the final least-squares cycle, are presented in Table II, while selected bond angles are given in Table III.

(31) Material supplementary to this article has been deposited as Document No. NAPS-00809 with the ASIS National Auxiliary Publication Service, c/o CCM Information Sciences, Inc., 909 Third Ave., New York, N. Y. 10022. A copy may be secured by citing the document number and remitting \$1.00 for microfiche or \$3.00 for photocopies. Advance payment is required. Make checks or money orders payable to: ASIS-NAPS.

The parameters of six important best planes in the molecular, together with distances of certain atoms from these planes, are given in Table IV.

If the 24 independent C-C bond distances of the phenyl rings are averaged, a standard deviation  $\sigma = [\sum(\bar{d} - di)^2 / (n - 1)]^{1/2}$  of 0.067 Å for an individual measurement is calculated. The maximum value of  $(\bar{d} - di)$  is 0.17 Å. Similarly, the maximum deviation of an individual carbon atom from the best planes A-F is 0.09 Å, and several other atoms deviate by 0.05-0.07 Å.

These errors are sufficiently large that variations in bond lengths involving carbon from accepted standard values cannot be regarded as significant. The inaccuracy arises because of the presence of three heavy atoms, and because sufficient high-order intensity data could not be gathered. The latter difficulty is in turn related to the moderately high thermal parameters of the structure. In addition, some systematic errors have undoubtedly crept into the data set by way of decomposition of the crystals in the X-ray beam. We note, moreover, that the corrections for absorption, extinction, and anomalous scattering did little to improve the final parameters.

**V. Unit Cell Parameters.** Cell constants have been established for compounds V, VI, and VII. These compounds crystallize in needles elongated on  $c$ . Weissenberg photographs indicate the three species to be isomorphous, and the reflection conditions  $0kl$ ,  $k + l = 2n$  and  $h0l$ ,  $h = 2n$  are consistent with space groups Pna2<sub>1</sub> and Pnam. Accurate cell constants have been determined by least-squares refinement of setting angles on the four-circle diffractometer (Mo K $\alpha$  radiation). These values are: Sn(CH<sub>3</sub>)<sub>2</sub>(C<sub>6</sub>H<sub>5</sub>)(C<sub>28</sub>H<sub>20</sub>Cl) (IV),  $a = 15.643$  (7),  $b = 12.073$  (4),  $c = 15.527$  (7); Sn(CH<sub>3</sub>)<sub>2</sub>(C<sub>6</sub>H<sub>5</sub>)(C<sub>28</sub>H<sub>20</sub>Br) (V),  $a = 15.890$  (3),  $b = 12.047$  (1),  $c = 15.563$  (3); Sn(CH<sub>3</sub>)<sub>2</sub>(C<sub>6</sub>H<sub>5</sub>)(C<sub>28</sub>H<sub>20</sub>I) (VI),  $a = 16.295$  (2),  $b = 12.156$  (2),  $c = 15.633$  (2) Å. The cell volume/density relationships indicate four molecules per unit cell. Space group Pnam would require molecular C<sub>2</sub> symmetry, which is inconsistent with the severe steric crowding of the dienes. Therefore space group Pna2<sub>1</sub> is indicated. X-Ray intensity data have been gathered on compound VI.

**Acknowledgment.** We are grateful to Francois van Remoortere for communicating preliminary structural data on compound VI. We are also pleased to acknowledge the contributions of Vernon R. Sandel and John J. Flynn to the earlier part of this work and some helpful discussions with S. W. Tobey, H. G. Langer, and J. W. Rakshys, Jr.

(32) J. Gvildy's version (ANL Program Library B-115) of Busing, Martin, and Levy's FORTRAN function and error program, OR-FFE, was used.

## Hydrogen and Trimethylsilyl Migrations in 5-Trimethylsilylcyclopentadiene

Arthur J. Ashe, III

Contribution from the Department of Chemistry,  
University of Michigan, Ann Arbor, Michigan 48104.

Received September 9, 1969

**Abstract:** 5-Trimethylsilyl-, 1-trimethylsilyl-, and 2-trimethylsilylcyclopentadiene were identified by nmr spectroscopy and formation of adducts with dimethyl acetylenedicarboxylate. The rate of hydrogen migration of 5-trimethylsilylcyclopentadiene is  $2.0 \times 10^{13} \exp(-26.2 \text{ kcal mole}^{-1}/RT)$ . This is 10<sup>6</sup> slower than trimethylsilyl migration.

5-Trimethylsilylcyclopentadiene exhibits a temperature dependent nmr spectrum.<sup>1</sup> At -10° the expected spectrum of a four-proton vinylic multiplet and one allylic proton signal is observed and at high temperature these signals coalesce into a single inter-

mediate frequency. It has been estimated that the ring protons are being interconverted at a rate of 10<sup>3</sup> sec<sup>-1</sup> at 80°.<sup>1</sup> According to one postulate, a series of 1,5-

(1) H. P. Fritz and C. G. Kreiter, *J. Organometal. Chem.*, **4**, 313 (1965).